Chinese Chemical Letters 31 (2020) 1686–1689

Contents lists available at ScienceDirect

Chinese Chemical Letters

journal homepage: www.elsevier.com/locate/cclet

Communication

A novel ferroelectric based on quinuclidine derivatives

Siyu Deng, Junyi Li, Xiang Chen, Yunlong Hou*, Lizhuang Chen*

School of Environmental and Chemical Engineering, Jiangsu University of Science and Technology, Zhenjiang 212003, China

ARTICLE INFO

Article history:
Received 26 September 2019
Received in revised form 3 November 2019
Accepted 7 November 2019
Available online 15 November 2019

Keywords:
Ferroelectric
Quinuclidine
Phase transition
Polarization
Dielectric

ABSTRACT

The compound $[(CH_3)_2CH\text{-}C_3H_{17}N][CoBr_4]$ (**1**) based on quinuclidine derivatives was achieved by the solution synthetic method and characterized by elemental analysis, infrared spectroscopy, single-crystal X-ray structural analysis and dielectric measurement, respectively. Variable-temperature single-crystal X-ray diffraction suggested that the compound underwent the phase transition from the space group *C2/c* to *Cc*. The polarization curve was measured using the Sawyer-Tower circuit. The structural phase transitions of **1** was ascribed to the distortion of a $[(CH_3)_2CH\text{-}C_3H_{17}N]^{2+}$ cation from this inorganic–organic hybrid material $[(CH_3)_2CH\text{-}C_3H_{17}N][CoBr_4]$. The strong change in dielectric anomalies makes compound **1** a suitable candidate for promising switchable dielectric materials. This work represents a feasible strategy thought for the targeted harvesting of low temperature ferroelectrics.

Phase transition materials are important functional materials with a variety of physical properties and potential application prospects [1–4]. Ferroelectric materials are a kind of special phase transition material [5–9]. They are widely used in large-capacity capacitors and optical information storage devices because of their dielectric, electro-optic and photorefractive effects [10–16]. At the same time, molecularly switchable dielectrics have received much attention due to their unique physical and chemical properties for signal processing sensing, data communications, solar cells and phase shifters [17–26]. It is highly necessary to discover more phase transition materials with outstanding physical properties and rich structure-property relationship. In the past, inorganic compounds (inorganic salts of metals and oxides) have attracted considerable attention as phase transition materials. One hot branch is molecular-based phase transition materials (organic molecules or organic-inorganic hybrids formed by the coordination or the recombination of metal ions), including compounds with 1-azadiracyclic[2.2.2] octane(quinuclidine) subunit [27–33]. In 2017, Xiong *et al.* reported a plastic crystal of quinuclidinium perrhenate ($HQReO_4$) through self-assembly of perrhenate and quinuclidine, then observed ferroelectricity in the temperature range from 298 K to 367 K [34]. In this study, 1-isopropyl-1-azabicyclo[2.2.2]octane, as the derivative of quinuclidine, was combined with metal halides, forming an inorganic–organic hybrid compound $[(CH_3)_2CH\text{-}C_3H_{17}N][CoBr_4]$ (**1**). The compound was synthesized and characterized. Differential scanning calorimetry, single crystal X-ray diffraction data and dielectric constant measurements detected that it transformed from a room-temperature phase with a space group of *C2/c* to a low-temperature phase with a space group of *Cc*. These findings indicate that the phase transition compound **1** has prominent switchable dielectric properties and provide evidence for the low temperature ferroelectricity.

The starting materials and reagents used throughout the experiments were of analytical grade from commercial sources and were used without any further purification. Infrared (IR) spectra were recorded on a SHIMADZU IR prestige-21 FTIR-8400S spectrometer in the range of 4000–500 cm^{-1} with samples in the form of potassium bromide pellets. Elemental analyses were taken on a Perkin-Elmer 240C elemental analyser. Powder X-ray diffraction (PXRD) measurements were made with a Rigaku SA-HFM3 diffraction system from $2\theta = 5°$ to $2\theta = 50°$ at 6 min^{-1} with an increment of 0.02° (Fig. S1 in Supporting information). Thermogravimetric analyses (TGA) were conducted on a TGA Q500 V20.13 Build 39 thermogravimeter with the heating rate of 10 K/min in a N_2 atmosphere (Fig. S2 in Supporting information). DSC analyses of crystal 1 (6.5 mg) was recorded using a Perkin Elmer Diamond DSC instrument in the range of −100 °C to 50 °C with a heating rate of 10 K/min on cooling/heating under nitrogen at atmospheric pressure in aluminum crucibles, respectively. The compound dielectric permittivity ($\varepsilon = \varepsilon' - i\varepsilon''$) was measured on a Tonghui TH2828A in the frequency range from 500 Hz to 1 MHz from –45 °C to 5 °C. A pellet sample was prepared at 10 MPa and the pressed powder pellet deposited with silver-conducting glue was used for the dielectric studies.

Crystallographic data of two compounds of appropriate size was collected at different temperatures on a Bruker SMART APEX-II

* Corresponding authors.
E-mail addresses: ylhou8@just.edu.cn (Y. Hou), clz1977@sina.com (L. Chen).

https://doi.org/10.1016/j.cclet.2019.11.011
1001-8417/

CCD diffractometer equipped with Mo-Kα radiation (λ = 0.71073 Å). Absorption correction is applied by using SADABS. The structures were resolved by a direct method and refined with full matrix least squares method using the SHELXTL-97 software package [35,36]. The distances and angles between some atoms are calculated using DIAMOND and other calculations are performed using SHELXLTL. All non-hydrogen atoms were refined with anisotropic thermal parameters. All hydrogen atoms attached to C, N and O atoms were added theoretically and refined with a riding model and fixed isotropic thermal parameters. The crystallographic data and details of collection and refining at different temperatures are given in Table 1.

In this work, the synthesis method is as follows: 1-Isopropyl-1-azabicyclo[2.2.2]octane (0.154 g, 1 mmol) and $CoBr_2$(0.22 g, 1 mmol) were mixed in deionized water solution (20 mL). After stirring, the mixture was allowed to stand at room temperature for 7 days to obtain compound **1** (Scheme S1 in Supporting information). IR data (KBr pellet, cm^{-1}): ν 3417(m), 2944(s), 2885(m), 1470(s), 1393(m), 1321(w), 1128(m), 845(m) (Fig. S3 in Supporting information). Anal. Calcd. (%) for $C_{10}H_{20}NBr_4Co$: C, 25.47; H, 4.59; N, 6.75. Found (%): C, 25.32; H, 4.61; N, 6.88.

It is well-known that DSC measurement is one of the useful thermodynamic methods to detect the dependence of reversible phase transition on temperature. When a compound undergoes structural phase transition accompanied by the thermal entropy change, heat anomalies can be observed during heating and cooling. DSC of compound **1** showed a main endothermic peak at −42 °C upon heating and a main exothermic peak on cooling at −47 °C (Fig. 1a). Through the heating curve of DSC, the enthalpy change of ΔH = 2.115 J/g, and the corresponding change in entropy enabled us to calculate, ΔS = 6.291 J mol^{-1} K^{-1}. Through the cooling curve of DSC, the enthalpy change of ΔH = 2.144 J/g, and the corresponding change in entropy enabled us to calculate, ΔS = 6.518 J mol^{-1} K^{-1}. Two main peaks and 5 °C of the thermal hysteresis show that compound **1** undergone a reversible phase transition. Meanwhile, such a second-order nature of the phase transition was also confirmed by the continuous change of second harmonic generation (SHG) intensity as a function of the temperature. As presented in Fig. 1b, the strong SHG signal at low temperature decreases gradually with the temperature increasing and finally disappears at around T_c. The disappeared SHG signal above Tc suggests a centrosymmetric phase while the detectable SHG signal below Tc indicates a non-centrosymmetric

Table 1
Crystallographic data for **1**.

Compound	$[(CH_3)_2CH\text{-}C_3H_{17}N][CoBr_4]$ (**1**)	
T (K)	296	170
Empirical formula	$C_{20}H_{40}N_2Br_4Co$	$C_{20}H_{40}N_2Br_4Co$
Formula weight	687.11	687.11
Crystal system	Monoclinic	Monoclinic
Space group	*C2/c*	*Cc*
a (Å)	13.044(13)	12.8050(3)
b (Å)	12.779(12)	12.6922(3)
c (Å)	16.122(15)	16.1330(4)
α(°)	90	90
β(°)	95.673(9)	96.668(2)
γ(°)	90	90
V (Å^3)	2674(4)	2604.26(11)
Z	4	4
D_c (g/m^3)	1.707	1.752
μ (mm^{-1})	6.627	6.805
F (000)	1364	1364
θ range [º]	2.647 to 24.997	2.507 to 25.344
Collected reflections	2352	4462
Unique reflections	1463	3812
R_1, wR_2 [I > 2σ (I)]	0.0622,0.1529	0.0401,0.0934
R_1, wR_2 [all data]	0.1131,0.1853	0.0526,0.1001
GOF	1.019	0.895

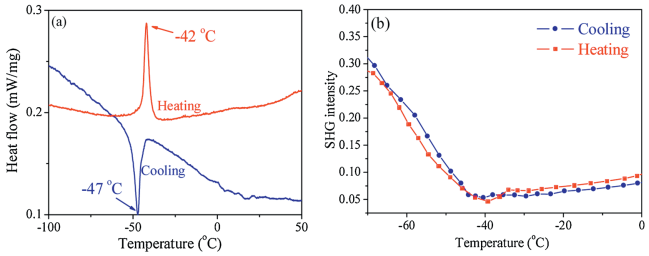

Fig. 1. (a) DSC curves of **1** obtained in a heating-cooling mode. (b) Temperature-dependent SHG intensity of **1**.

one, consistent with the symmetry breaking transition from space group *C2/c* at RTP to *Cc* at LTP. In addition, the cell parameters of **1** was measured at different temperatures (Fig. S4 in Supporting information), which was consistent with the results of DSC measurement.

A standard Sawyer-Tower circuit was employed to measure the polarization as a function of external electric field. As shown in Fig. 2, P-E loops at different temperatures are well presented, affording indispensable proof for the low temperature ferroelectricity of **1**. Besides, the film of **1** shows a considerable remnant polarization with a value of 0.19 μC/cm^2 at −44 °C. In order to obtain a proper loop, the film thickness has to be very small (<5 μm) so the applied bias voltage can overcome the large coercive potential.

In addition, the specific variable temperature structures of RTP and LTP were measured, respectively. The phase transition of **1** was further confirmed by determining the crystal structures at 296 K and 200 K, respectively. In RTP (296 K), the crystals are in the monoclinic space group with the centrosymmetric space group *C2/c* and the point group C_{2h}. When cooled to 170 K, the crystals are in the non-centrosymmetric space group *Cc* and the point group C_3. The molecular volume decreased from 2674(4) Å^3 in *C2/c* to 2604.26(11) Å^3 in *Cc*. In the room-temperature phase (RTP) (296 K), the asymmetric unit of **1** includes two $[(CH_3)_2CH\text{-}C_3H_{17}N]^+$ cations and a tetrahedral $[CoBr_4]^{2-}$ anion (Fig. 3a). The Co(II) ion is in a slightly distorted octahedral environment with four Cl atoms. The bond distances of Co1–Br1, Co1–Br3, Co1–Br1$^{\#1}$ and Co1–Br3$^{\#1}$ (symmetry codes: #1: -x, y, 0.5−z) are 2.4084(19) Å, 2.3894(20) Å, 2.4084(19) Å and 2.3894(20) Å, respectively, and the bond angles of Br–Co–Br vary from 104.000(48)° to 113.222(41)°, which are comparable to the reported values [37–39]. In the asymmetric unit of the RTP structure, one non-hydrogen atom (Co1) was located in a mirror plane with an occupancy factor of 0.5 (Fig. S5a in Supporting

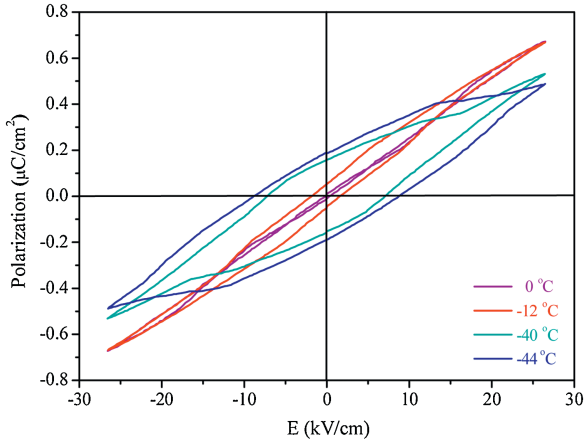

Fig. 2. Voltage dependence of the spontaneous polarization at various temperatures, measured from a Sawyer – Tower circuit.

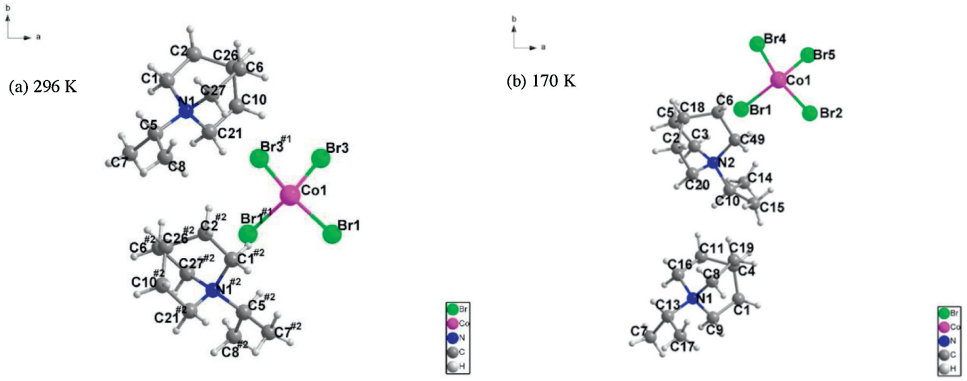

Fig. 3. View of the coordination environment of **1** with atomic numbering scheme at (a) 296 K, symmetry codes: #1: -x, y, 0.5−z; #2: -0.5−x, -0.5+ y, 0.5−z; (b) 170 K.

information), while others apart from the above mirror plane can be produced by (-x, y, 0.5−z) and (-0.5−x, -0.5+ y, 0.5−z) symmetry transformation.

In the low-temperature phase (LTP) (170 K), the asymmetric unit of **1** includes two $[(CH_3)_2CH\text{-}C_3H_{17}N]^+$ cations and a tetrahedral $[CoBr_4]^{2-}$ anion just like at room temperature, the Co(II) ion also adopts a distorted tetrahedral geometry (Fig. 3b). The bond distances of Co1–Br1, Co1–Br2, Co1–Br4 and Co1–Br5 are 2.4132(16) Å, 2.4210(16) Å, 2.3983(18) Å and 2.4030(19) Å, respectively, and the bond angles of Br–Co–Br vary from 104.919 (61)° to 113.841(66)°, which are slightly different from those in RTP. In the LTP unit cell, non-hydrogen atoms apparently deviated from the crystallographic mirror plane (Fig. S5b in Supporting information). Meanwhile, the conformations of the rings of the quinuclidine ligand showed some differences between the two phases. The torsion angle of N–C–C–N in quinuclidine rings varies from 0.09° to 1.97° at 296 K. Moreover, N–C–C–N exhibited large twisting conformations with the torsion angles from -6.35° to 11.17° at 170 K, suggesting that the rings were seriously distorted compared with those in RTP. This indicates that the quinuclidine ring of the $[(CH_3)_2CH\text{-}C_3H_{17}N]^+$ cation differs in the temperature variation. With the disappearance of partial symmetry codes, the Co–Br distances and bond angles of Br–Co–Br are slightly different from RTP (Table S1 in Supporting information).

The distances of adjacent Co metals along *b* axis have been studied in order to further demonstrate the structural differences between the room temperature phase and the low temperature phase. At room temperature, six Co metals can be seen along the *b*-axis. The bonds of Co···Co were connected to study the differences between different temperatures. As shown in Fig. S6a (Supporting information), there were two kinds of distances of adjacent Co, which were 9.1304 Å and 9.6747 Å. When the temperature was cooled, the position of the center Co metals was changed along the direction of the arrow. As the temperature dropped below T_c (Fig. S6b in Supporting information), the distances of adjacent Co···Co changed for three kinds, which were 9.0147 Å, 9.7769 Å and 10.7912 Å. The positions of the cobalt atoms changed at different temperatures, which further proved the occurrence of phase transition.

Dielectric constant (both real part ε' and dielectric loss) undergoes abrupt changes in the vicinity of the phase transition (T_c), while the magnitude of the variations was related to the characteristics of such transition [40–50]. The dielectric permittivity of **1** was measured in the frequency range between 500 Hz and 1 MHz in cooling and heating modes. In order to obtain more accurate data, we used a large crystal with a smooth surface instead of powder pellet to conduct the dielectric test. As illustrated in Fig. S7a (Supporting information), the real part (ε') of dielectric constants distinctly experienced an obvious dielectric transition on the heating and cooling progress at 1 MHz. Dielectric transitions can be seen between −16 °C and −14 °C. Compared with the DSC image, the dielectric response is delayed, which is subject to the DSC image. Fig. S7b (Supporting information) is a temperature dependent curve of dielectric loss of compound **1** at a frequency of 1 MHz. Such a dielectric anomaly indicated that it has undergone a phase transition.

In summary, a low temperature ferroelectric phase transition compound $[(CH_3)_2CH\text{-}C_3H_{17}N][CoBr_4]$ was successfully achieved. Variable-temperature structural analysis, DSC and dielectric measurements revealed that compound **1** underwent reversible low-temperature phase transition at around 228 K. Single crystal X-ray diffraction demonstrated that compound **1** crystallizes in the orthorhombic space group *C2/c* at RTP and in the monoclinic space group *Cc* at LTP. The dynamics of the quinuclidine ring of the $[(CH_3)_2CH\text{-}C_3H_{17}N]^+$ cation played an essential role in the mechanism of the phase transition. The change of the dielectric permittivity and the spontaneous polarization behavior highlight the great potential of compound **1** as low temperature ferroelectrics.

Declaration of competing interest

The authors declare that they have no known competing financial interests or personal relationships that could have appeared to influence the work reported in this paper.

Acknowledgments

This work was financially supported by the National Natural Science Foundation of China (No. 21671084), NSF of Jiangsu Province (No. BK20131244), Six talent peaks project in Jiangsu Province (No. 2014-XCL-008), the Qing Lan Project of Jiangsu Province, the Innovation Program of Graduate Students in Jiangsu Province (No. KYLX16-0508), a Project Funded by the Priority Academic Program Development of Jiangsu Higher Education Institution, Innovation Program for Graduate Student from Jiangsu University of Science and Technology (No. YCX15S-19) and the Foundation of Jiangsu Educational Committee (No. 16KJB430011).

Appendix A. Supplementary data

Supplementary material related to this article can be found, in the online version, at doi:https://doi.org/10.1016/j.cclet.2019.11.011.

References

[1] H.Y. Ye, W.Q. Liao, C.L. Hu, et al., Adv. Mater. 28 (2016) 2579–2586.
[2] M. Salinga, M. Wuttig, Sci. 332 (2011) 543–544.

[3] X. Chen, H. Zhou, Y.Y. Chen, A.H. Yuan, CrystEngComm 13 (2011) 5666–5669.
[4] H.Y. Ye, H.L. Cai, J.Z. Ge, R.G. Xiong, Inorg. Chem. Commun. 17 (2012) 159–162.
[5] Q. Pan, Z.B. Liu, Y.Y. Tang, et al., J. Am. Chem. Soc. 139 (2017) 3954–3957.
[6] W.Q. Liao, Y.Y. Tang, P.F. Li, Y.M. You, R.G. Xiong, J. Am. Chem. Soc. 139 (2018) 3954–3957.
[7] Z.H. Sun, X.Q. Wang, J.H. Luo, et al., J. Mater. Chem. C 1 (2013) 2561–2567.
[8] X.N. Hua, W.Q. Liao, Y.Y. Tang, et al., J. Am. Chem. Soc. 140 (2018) 12296–12302.
[9] W. Zhang, H.Y. Ye, H.L. Cai, et al., J. Am. Chem. Soc. 132 (2010) 7300–7302.
[10] C.Y. Mao, W.Q. Liao, Z.X. Wang, et al., Inorg. Chem. 55 (2016) 7661–7666.
[11] Y.Z. Tang, B. Wang, H.T. Zhou, et al., Inorg. Chem. 57 (2018) 1196–1202.
[12] H.P. Chen, P.P. Shi, Z.X. Wang, et al., Dalton Trans. 47 (2018) 7005–7012.
[13] Y.W. Zhang, P.P. Shi, W.Y. Zhang, Q. Ye, D.W. Fu, Inorg. Chem. 57 (2018) 10153–10159.
[14] L.B. Kong, S. Li, T.S. Zhang, J.W. Zhai, F.Y.C. Boey, J. Prog. Mater. Sci. 55 (2010) 840–893.
[15] Y. Liu, H.T. Zhou, S.P. Chen, et al., Dalton Trans. 47 (2018) 3851–3856.
[16] Y. Zhang, H.Y. Ye, H.L. Cai, et al., Adv. Mater. 26 (2014) 4515–4520.
[17] P.E. Carbonneau, S.N. Lane, N. Bergeron, Earth Surf. Processes Landforms 31 (2006) 1413–1423.
[18] C. Shi, X. Zhang, Y. Cai, Y.F. Yao, W. Zhang, Angew. Chem. Int. Ed. 54 (2015) 6206–6210.
[19] W. Zhang, Y. Cai, R.G. Xiong, H. Yoshikawa, K. Awaga, Angew. Chem. Int. Ed. 49 (2010) 6608–6610.
[20] A. Vorobiev, P. Rundqvist, K. Khamchane, S. Gevorgian, Appl. Phys. Lett. 83 (2003) 3144–3146.
[21] D.H. Cao, C.C. Stoumpos, O.K. Farha, J.T. Hupp, M.G. Kanatzidis, J. Am. Chem. Soc. 137 (2015) 7843–7850.
[22] W. Zhang, H.Y. Ye, R. Graf, et al., J. Am. Chem. Soc. 135 (2013) 5230–5233.
[23] C. Shi, C.H. Yu, W. Zhang, Angew. Chem. 128 (2016) 5892–5896.
[24] A.B. Ustinov, G. Srinivasan, B.A. Kalinikos, Appl. Phys. Lett. 90 (2007) 031913–031913.
[25] F. Hao, C.C. Stoumpos, R.P.H. Chang, M.G. Kanatzidis, J. Am. Chem. Soc. 136 (2014) 8094–8099.
[26] N.J. Jeon, J.H. Noh, Y.C. Kim, et al., Nat. Mater. 13 (2014) 897–903.
[27] L.Z. Chen, D.D. Huang, Q.J. Pan, J.Z. Ge, F.M. Wang, CrystEngComm 16 (2014) 2944–2949.
[28] L.Z. Chen, D.D. Huang, J.Z. Ge, Q.J. Pan, J. Mol. Struct. 1072 (2014) 307–312.
[29] L.Z. Chen, D.D. Huang, Q.J. Pan, L. Zhang, J. Mol. Struct. 1078 (2014) 68–73.
[30] L.Z. Chen, Q. Ji, X.G. Wang, Q.J. Pan, X.X. Cao, CrystEngComm 19 (2017) 5907–5914.
[31] C.H. Chen, G.C. Xu, CrystEngComm 18 (2016) 550–557.
[32] K. Gao, C. Liu, Z. Cui, et al., J. Mater. Chem. C 4 (2016) 1959–1963.
[33] Y. Zhang, W. Zhang, S.H. Li, et al., J. Am. Chem. Soc. 134 (2012) 11044–11049.
[34] Y.Y. Tang, P.F. Li, P.P. Shi, et al., Phys. Rev. Lett. 119 (2017) 207602.
[35] G.M. Sheldrick, SHELXL-97, Program for Crystal Structure Solution, University of Gottingen, Germany, 1997.
[36] G.M. Sheldrick, SHELXS-97, Program for Crystal Structure Refinement, University of Gottingen, Germany, 1997.
[37] L.Z. Chen, X.X. Cao, D.D. Huang, Q.J. Pan, RSC Adv. 5 (2015) 55914–55919.
[38] L.Z. Chen, D.D. Huang, Q.J. Pan, J.Z. Ge, RSC Adv. 5 (2015) 13488–13494.
[39] L.Z. Chen, X.X. Cao, Q.J. Pan, Q. Ji, Chem. Select. 1 (2016) 6499–6506.
[40] D.H. Wu, L. Jin, Y. Zhang, Inorg. Chem. Commum. 23 (2012) 117–122.
[41] Q. Ji, L.H. Li, S.Y. Deng, X.X. Cao, L.Z. Chen, Dalton Trans. 47 (2018) 5630–5638.
[42] Y. Zhang, K. Awaga, H. Yoshikawab, R.G. Xiong, J. Mater. Chem. 22 (2012) 9841–9845.
[43] L.H. Li, W.Y. Zhao, S.Y. Deng, L.F. Ma, L.Z. Chen, Inorg. Chem. Commum. 92 (2018) 125–130.
[44] L.Z. Chen, Q. Ji, Y.Y. Dan, Chin. J. Struct. Chem. 35 (2016) 1728–1735.
[45] Q. Li, P.P. Shi, Q. Ye, et al., Inorg. Chem. 54 (2015) 10642–10647.
[46] L.Z. Chen, J. Sun, Q. Ji, Q.J. Pan, Y. Huang, Chin. J. Struct. Chem. 36 (2017) 329–337.
[47] Y. Zhang, K. Awaga, H. Yoshikawab, R.G. Xiong, J. Mater. Chem. 22 (2012) 9841–9845.
[48] L.H. Kong, D.W. Fu, Q. Ye, et al., Chin. Chem. Lett. 25 (2014) 844–848.
[49] M.A. Asghar, J. Zhang, S.G. Han, et al., Chin. Chem. Lett. 29 (2018) 285–288.
[50] Z.H. Yan, X.Y. Li, L.W. Liu, et al., Inorg. Chem. 55 (2016) 1096–1101.